Carbohydrate Polymers 94 (2013) 170–178

Contents lists available at SciVerse ScienceDirect

Carbohydrate Polymers

journal homepage: www.elsevier.com/locate/carbpol

Ice-templated hydrogels based on chitosan with tailored porous morphology

Maria Valentina Dinu[a], Martin Přádný[b], Ecaterina Stela Drăgan[a,*], Jiří Michálek[b]

[a] "Petru Poni" Institute of Macromolecular Chemistry, Aleea Grigore Ghica Voda 41 A, RO-700487 Iasi, Romania
[b] Institute of Macromolecular Chemistry, Academy of Sciences of the Czech Republic, Heyrovský Sq 2, Prague 6, Czech Republic

ARTICLE INFO

Article history:
Received 21 August 2012
Received in revised form
14 November 2012
Accepted 13 January 2013
Available online 4 February 2013

Keywords:
Chitosan
Ice-templated hydrogels
Morphology
Unidirectional freezing

ABSTRACT

Preparation and morphological characterization of some novel hydrogels based on chitosan (CS) with porous structure tailored by ice-templating and porogen leaching are presented in the paper. Poly(methylmethacrylate) (PMMA), as fractionated particles, has been used as polymer porogen. The influence of the mesh of the fractionated PMMA particles, the weight ratio between CS and fractionated PMMA particles, and the speed of the crystallization, on the internal morphology of the hydrogels have been deeply investigated. The morphology of the obtained hydrogels was observed by scanning electron microscopy (SEM). As a function of the synthesis conditions, hydrogels with a heterogeneous morphology consisting of randomly and evenly distributed polyhedral pores, or with an oriented structure, which has microchanneled structures arranged along the freezing direction, were generated.

1. Introduction

Considerable interest has been lately focused on the designing of novel porous hydrogels with controlled morphology and increased levels of spatial organization and functionalities (Chang, Duan, & Zhang, 2009; Dragan, Perju, & Dinu, 2012; Kirsebom, Topgaard, Galaev, & Yu Mattiasson, 2010; Zhao, Sun, Wu, & Lin, 2011). Porous hydrogels have found more benefits than conventional hydrogels when they are used as chromatographic materials (Lozinsky, Plieva, Galaev, & Mattiasson, 2001), controlled delivery devices for drugs and proteins (Bajpai, Shukla, Bhanu, & Kankane, 2008; Peppas, Hilt, Khademhosseini, & Langer, 2006; Reis et al., 2008), matrices for the immobilization and separation of molecules and cells (Baydemir et al., 2009; Hobzova et al., 2011; Savina et al., 2007), and matrices for repairing and regenerating a wide variety of tissues and organs (Dispinar, Van Camp, De Cock, De Geest, & Du Prez, 2012; Kathuria, Tripathi, Kar, & Kumar, 2009; Shapiro & Cohen, 1997). Hydrogels designed for use as scaffolds in tissue engineering may contain pores large enough to accommodate living cells, or they may be designed to dissolve or degrade away, releasing growth factors and creating pores into which living cells may penetrate and proliferate. In our previous work (Lesný et al., 2006), we observed that cell growth on the gel scaffold was reduced, or even stopped after some time, this fact being explained by the limited nutrient supply as the large pores became blocked with cells. Therefore, the objective of this study was to design tailored porous hydrogels (pore size on the order of tens to hundreds of μm), with less compact walls between the large pores. The permeable walls would allow the freely diffusion of low-molar mass substances, when the large pores are filled by cells.

To achieve permanent porosity within three-dimensional polymer networks, various methods have been reported, such as: (1) cross-linking polymerization in the presence of a pore-forming agent, when a microphase separation occurs (Sayil & Okay, 2001), (2) cross-linking polymerization in the presence of water-soluble substances (sugars, salts, polymers), which are washed out from the hydrogel after polymerization (Přádný et al., 2003; Přádný, Šlouf, Martinová, & Michálek, 2010), (3) cross-linking in the presence of substances releasing porogen gases (Kim & Park, 2004), (4) lyophilization of the hydrogel swollen in water (Dragan, Cazacu, & Nistor, 2009), and (5) ice-templating process (cryogelation) (Chang et al., 2009; Dinu, Ozmen, Drăgan, & Okay, 2007; Dinu, Perju, & Drăgan, 2011a; Dinu, Perju, & Drăgan, 2011b; Dispinar et al., 2012; Gutiérrez, Ferrer, & del Monte, 2008; Kathuria et al., 2009; Kirsebom et al., 2010; Lozinsky, 2002; Savina et al., 2007; Zhao et al., 2011), which is a special method derived from the method (2), where the ice crystals are the solid porogen. In the ice-templating process, the soluble substances (monomers, initiator, polymers) originally dissolved in the aqueous medium are expelled from the forming ice and concentrated within the non-frozen liquid channels between adjacent ice crystals. The cross-linking polymerization occurs in these non-frozen channels, the ice crystals acting as a template during gelation, their removal after thawing leading to a system with large and interconnected pores. Hydrogels with highly

* Corresponding author. Tel.: +40 232 217454; fax: +40 232 211299.
E-mail address: sdragan@icmpp.ro (E.S. Drăgan).

0144-8617/$ – see front matter © 2013 Elsevier Ltd. All rights reserved.
http://dx.doi.org/10.1016/j.carbpol.2013.01.084

interconnected porous networks designed by this method are called cryogels. In addition to the interconnected macroporous structure, cryogels possess a tissue-like elasticity, are able to withstand high levels of deformations, such as elongation and torsion, being also characterized by superfast responsiveness at water absorption (Dinu et al., 2007, 2011b; Kirsebom et al., 2010; Orakdogen, Karacan, & Okay, 2011). A number of authors have demonstrated the capacity of ice-templating process to control the morphology of the resulting macroporous structures by unidirectional freezing technique at a controlled immersion rate (Gutiérrez et al., 2008; Hu, Shen, Yang, Bei, & Wang, 2008; Kim, Taki, Nagamine, & Ohshima, 2009; Mukai, Nishihara, & Tamon, 2008; Wu, Zhao, Sun, & Zhou, 2012). In this approach, different systems such as aqueous polymer solutions, inorganic colloidal dispersions or their hybrid composites are unidirectionally frozen in some freezing agents like liquid nitrogen (−196 °C), frozen ethanol (−110 °C) or frozen acetic acid and ethylether (−80 °C) and so the ice crystals (or solvent crystals) form and grow unidirectionally. This process achieves microchanneled structures which are well-aligned in the freezing direction with a well-patterned between channel morphology (e.g., micro-honeycomb or lamellar). Unidirectional freezing technique has been used to prepare aligned silica fibers (Mukai et al., 2008), aligned porous structure from water-soluble polymers such as poly(vinyl alcohol) (Gutiérrez et al., 2008), poly(L-lactic acid) (Kim et al., 2009), poly(lactide-co-glycolide) (Hu et al., 2008), and recently poly(ethylene glycol) aligned porous cryogels (Wu et al., 2012).

In the present paper, the design of two types of chitosan (CS) cryogels with tailored porous morphology by the synthesis conditions is developed. The choice of CS was based on its hydrophilic, biocompatible, and biodegradable properties, which provides to the hydrogel potential applications in biomedical, pharmaceutical, and environmental fields (Kathuria et al., 2009; Ji, Annabi, Khademhosseini, & Dehghani, 2011; Takei, Nakahara, Ijima, & Kawakami, 2012; Zhao et al., 2011). One type of cryogel presented a heterogeneous morphology consisting of randomly and evenly distributed polyhedral pores, produced by a strategy which combines ice-templating process and porogen leaching. Besides the formation of interconnected pores by cryogelation, poly(methylmethacrylate) (PMMA), as fractionated particles, has been used as polymer porogen, which was washed out by acetone from the hydrogel after reaction. The other type exhibited an oriented structure, which walls were arranged along the freezing direction, obtained by a strategy which combines unidirectional freezing at −196 °C, −28 °C, and −13 °C, ice-templating process and porogen leaching. To the best of our knowledge, there are no cryogels based on CS synthesized by the strategies proposed in this work. The morphology of the obtained cryogels was observed by scanning electron microscopy (SEM). The effects of the mesh of the fractionated PMMA particles, the weight ratio between CS and fractionated PMMA particles, and speed of the crystallization on the pore structure of CS cryogels were investigated.

2. Materials and methods

2.1. Materials

The CS with molar mass of 467 kDa (CS), purchased from Sigma–Aldrich, was used as received. The intrinsic viscosity of CS solved in the mixture of 0.3 M acetic acid and 0.2 M sodium acetate (1:1, v/v) was measured with an Ubbelohde viscometer at 25 ± 0.1 °C. The viscometric average molar mass of CS was estimated using Eq. (1) (Gamzazade et al., 1985):

$$[\eta] = 1.38 \times 10^{-4} M_v^{0.85} \quad (1)$$

Degree of acetylation (DA) of CS was evaluated by infrared spectroscopy using a Vertex 70 Bruker FTIR spectrometer. Transmission spectra were recorded in KBr pellets. For DA determination, Eq. (2) was used, taking the 1420 cm^{-1} band as reference and as characteristic band for the N-acetylglucosamine the band located at 1320 cm^{-1} (Brugnerotto et al., 2001):

$$\frac{A_{1320}}{A_{1420}} = 0.3822 + 0.03133\mathrm{DA} \quad (2)$$

An average value of DA = 15%, resulted from three measurements, was taken into account. Glutaraldehyde (GA) as aqueous solution with a concentration of 25%, purchased from Sigma–Aldrich, was used as received. PMMA, prepared as fractionated particles with mesh below 32 μm, 32–50 μm, and 50–90 μm, has been used as second porogen which was washed out from the CS matrix by acetone.

2.2. Preparation of cryogels

Cryogels were prepared as monoliths by cross-linking CS with GA below the freezing point of the reaction solution at −18 °C (ice-templating technique) in the presence of the fractionated PMMA particles. Parameters which have been varied in the synthesis of CS cryogels were: mesh of the fractionated PMMA particles, weight ratio between CS and fractionated PMMA particles, and speed of crystallization. The weight ratio CS:PMMA was ranged from 1:0.5 to 1:30, and fractionated PMMA particles with three fractions of mesh below 32 μm, 32–50 μm, and 50–90 μm have been used. A CS solution with a concentration of 2 wt% was prepared by adding 2 g CS powder in 100 mL 1 vol% acetic acid solution and stirring for 24 h at room temperature. GA was used as aqueous solution with a concentration of 2.5%. CS and GA solutions were first incubated at 4 °C. After that, 10 mL of CS solution (2%) were mixed with 0.42 mL of GA solution (2.5%). The mixed solutions were cooled to 0 °C and kept on a mechanical rotor for 30 min. PMMA, as fractionated particles, was then added into CS and GA mixed solutions and was thoroughly mixed for 5 min. Thorough mixing of the components produced a paste that was divided into two portions and was transferred into the chambers of two pelleting devices, previously described (Přádný et al., 2003). The chambers were closed by a flange with fastening screws and the tightening screw was tightened in a standard way with a moment of force of 10 Nm. The first pelleting device was directly incubated into a freezer at −18 °C for 24 h. In order to see the effect of speed of crystallization on the morphology of CS cryogels, the second pelleting device was firstly kept closely at the surface of a freezing agent, such as liquid nitrogen (−196 °C), or ethylene glycol (−28 °C and −13 °C) being well fixed in order to maintain its bottom close to the surface of the freezing agent. After the freezing of reaction mixture completely (less than 5 min for liquid nitrogen, about 15 min at −28 °C, and about 40 min at −13 °C,), the pelleting device was also transferred into a freezer to complete the cross-linking of CS at −18 °C for 24 h.

After 24 h of incubation at −18 °C, the pelleting devices were taken out and were maintained at room temperature for 1 h. After that, the samples from the chambers of the pelleting devices were carefully taken out and were repeatedly immersed in a large excess of acetone to wash out the fractionated PMMA particles. Each sample was washed with acetone 5–14 days, depending on the mesh and weight ratio CS:PMMA and finally with a series of water–acetone mixtures with increasing water contents (vol.%), as follows: 20% (6 h) → 40% (6 h) → 60% (6 h) → 80% (6 h) → 100% (24 h). Thereafter, the swollen cryogel samples were frozen in liquid nitrogen, and lyophilized (24 h, at −57 °C and 0.045 mbar), the drying effect on the cryogel morphology in swollen state being thus leveled off. As control, CS cryogel (2%) without fractionated

Table 1
The samples code, the experimental parameters and the freezing conditions varied during the synthesis of CS cryogels.

Sample code	CS conc. (%)	GA conc. (%)	PMMA particle mesh (μm)	Weight ratio CS:PMMA	Freezing temperature[a] (°C)	Freezing duration[b] (min)
CS			–	–	−18	30
CS0.5.32			0–32	1:0.5	−18	30
CS2.32			0–32	1:2	−18	30
CS6.32			0–32	1:6	−18	30
CS12.32			0–32	1:12	−18	30
CS25.32			0–32	1:25	−18	30
CS30.32			0–32	1:30	−18	30
CSLN			–	–	−196	Less than 5
CS12.32LN	2	2.5	0–32	1:12	−196	Less than 5
CS4.50			32–50	1:4	−18	30
CS12.50			32–50	1:12	−18	30
CS4.90			50–90	1:4	−18	30
CS12.90			50–90	1:12	−18	30
CS12.90LNi[c]			50–90	1:12	−196	Less than 1
CS12.90EG			50–90	1:12	−28	15
CS12.90EG			50–90	1:12	−13	40
CS18.90			50–90	1:18	−18	30

[a] The freezing temperature or the speed of crystallization of the reaction mixture indicates which samples were pre-treated with freezing agents (liquid nitrogen = LN; ethylene glycol = EG).
[b] The freezing duration represents the time in which the freezing of reaction mixture was completely.
[c] CS12.90LNi has been synthesized by pre-frozen of the initial reaction mixture by dipping in liquid nitrogen.

PMMA particles was also synthesized to compare their properties with CS cryogel prepared in the presence of PMMA as template.

The feed composition, the freezing conditions and the samples code of the CS cryogels are summarized in Table 1.

The general code of CS cryogels consists of the term CS followed by two numbers separated by dot: the first one represents the weight ratio of PMMA to CS, and the second one represents the upper mesh of the fractionated PMMA particles. For samples prepared by frozen of the initial reaction mixture using freezing agents, the general code includes also the term LN for liquid nitrogen and EG for ethylene glycol (Table 1).

2.3. Characterization of cryogels

2.3.1. Morphological analysis

Surface morphology and internal structure of the dried cryogels were observed using an environmental scanning electron microscope (ESEM) type Quanta 200, in low vacuum mode. The cross-sections of the samples were performed using a sharp blade to revel the internal structures.

2.3.2. Porosity

The swollen state porosity of the networks, P_s (%), which represents the percentage of spaces or voids (pores) within a solid material in swollen state, was estimated from the equilibrium volume and the equilibrium weight swelling ratios of the CS cryogels, using Eq. (3) (Dinu et al., 2007).

$$P_s = \left[1 - q_v\left(1 + \frac{(q_w - 1)d_2}{d_1}\right)^{-1}\right] \times 100 \quad (3)$$

where q_v is the equilibrium volume swelling ratios, q_w is the equilibrium weight swelling ratios, d_1 is the density of solvent (water) and d_2 is the density of CS (0.6 g/cm^3) (Aranaz et al., 2009).

The equilibrium volume (q_v) and the equilibrium weight swelling ratios (q_w) of the cryogels, were calculated as:

$$q_v = \left(\frac{D_w}{D_{dry}}\right)^3 \quad (4)$$

$$q_w = \frac{m_w}{m_{dry}} \quad (5)$$

where D_w and D_{dry} are the diameters of the equilibrium swollen and dry gels and were measured by a calibrated digital compass, m_w and m_{dry} are the weight of gels after equilibrium swelling in water and after drying, respectively.

The dry-state porosity of the networks, P (%), which represents the percentage of spaces or voids (pores) within a solid material in dry state, was estimated from their densities. For this purpose, the weights m_{dry}, m_w and the dimensions (diameters D_{dry}, D_w and lengths l_{dry}, l_w) of cylindrical CS cryogels were measured, from which the densities were calculated with Eqs. (6) and (7) (Dinu et al., 2007):

$$d_0 = \frac{m_{dry}}{(\pi D_{dry}^2 l_{dry}/4)}, \quad \text{g mL}^{-1} \quad (6)$$

$$d_3 = \frac{m_w}{(\pi D_w^2 l_w/4)}, \quad \text{g mL}^{-1} \quad (7)$$

The total porosity P (%) was calculated as follows:

$$P = \left(1 - \frac{d_0}{d_3}\right) \times 100 \quad (8)$$

where d_0 is the density of the dried cross-linked polymer and d_3 is the density of the equilibrium swollen cross-linked polymer.

The volume fraction of pores in cryogel (V_p) was also evaluated by Eq. (9):

$$V_p = 1 - \frac{m}{d_2 V_T} \quad (9)$$

where m is the weight of dry phase (CS + GA); d_{CS} is the density of CS (0.6 g/cm^3); V_T is the total volume of hydrogel (in water) calculated for the cylindrical shape of sample, as:

$$V_T = \pi\left(\frac{D_w}{2}\right)^2 l_w \quad (10)$$

3. Results and discussion

CS cryogels with tailored porous structure were synthesized at −18 °C by two strategies: one combines ice-templating process and porogen leaching technique, and the other one combines unidirectional freezing at −196 °C, −28 °C, and −13 °C, ice-templating process and porogen leaching technique. It is well known that the formation and strength of the cryogels are affected by a series of factors, such as molecular weight of polymer, concentration, gel preparation temperature, thawing temperature, thawing rate, freezing duration and the number of freeze–thawing cycles, etc. (Lozinsky, 2002). The gel preparation temperature −18 °C has been

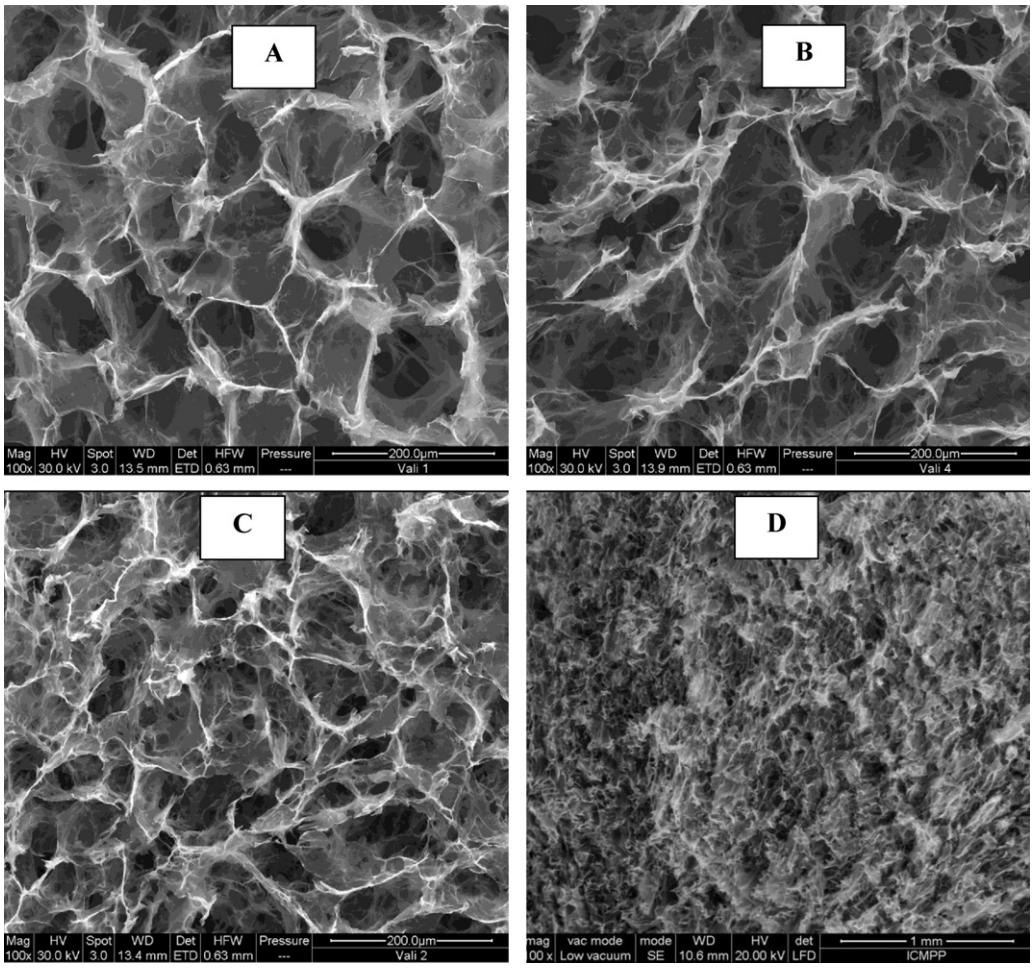

Fig. 1. SEM micrographs of the CS cryogels prepared by conventional ice-templating process with a weight ratio between CS and PMMA of 1:12, different only by the mesh of the fractionated PMMA particles: (A) CS12.32, (B) CS12.50 and (C) CS12.90. Image (D) presents the internal morphology of the CS12.90 cryogel prepared by dipping the initial reaction mixture in liquid nitrogen. The magnification is 100×.

chosen because the previous studies concerning the formation of PAAm cryogels showed that cryogels with enhanced mechanical properties and largest pores of sizes about 70 μm could be obtained (Dinu et al., 2007, 2011a, 2011b). GA was used as aqueous solution with a concentration of 2.5% in the preparation of CS cryogels, because this concentration of GA proved to be efficient in preparing composite hydrogels based on chitosan and poly(N-2-aminoethyl acrylamide) (Dragan & Perju, 2010).

The influence of the mesh of PMMA fractionated particles, the weight ratio between CS and fractionated PMMA particles, and the pre-freezing temperature of the initial reaction mixture or the speed of crystallization on the internal morphology of the CS cryogels will be evaluated in the following sections.

3.1. Effect of the mesh of the fractionated PMMA particles on pore structure of cryogels

The morphology of CS cryogels prepared by conventional ice-templating process in the presence of the fractionated PMMA particles with different mesh has been examined by SEM. SEM images of CS cryogels presented in Fig. 1 support the morphological changes occurring in the structure of CS cryogels when they are prepared in the presence of the fractionated PMMA particles with mesh below 32 μm (Fig. 1A), 32–50 μm (Fig. 1B) and 50–90 μm (Fig. 1C).

As can be observed, besides the decreasing of the pore size, strong changes occurred in the morphology of the walls of CS cryogels prepared in the presence of the fractionated PMMA particles with mesh of 50–90 μm (CS12.90, Fig. 1C). The pore walls are less compact and therefore, more accessible for the diffusion of low molecular weight species than those of CS cryogels prepared in the presence of the fractionated PMMA particles with mesh below 32 μm (CS12.32, Fig. 1A) or 32–50 μm (CS12.50, Fig. 1B). This shows that, the fractionated PMMA particles with mesh of 50–90 μm had a strong influence on the morphology of the pore walls of CS network. Thus, the increase of the fractionated PMMA particles mesh, for the same weight ratio between CS and PMMA (1:12), conducted to a decrease of the pores sizes from 84 ± 6 μm to 60 ± 4 μm, as well as to an increase of the number of the interconnected small pores of cryogels (Fig. 1C compared with Fig. 1A and B). Moreover, the pre-freezing of the initial reaction mixture by dipping in liquid nitrogen had two consequences: a more uniform pore size distribution, and the decrease of the pore sizes at 30 ± 4 μm for CS12.90LNi cryogel (Fig. 1D).

3.2. Effect of weight ratio CS:PMMA on pore structure of cryogels

The effect of the weight ratio between CS and PMMA on the morphology of the CS cryogels prepared by conventional ice-templating cross-linking was investigated using the following ratios CS/PMMA: 1:0.5, 1:2, 1:6, 1:12, 1:25 and 1:30. Fig. 2 shows the internal morphology of the CS cryogels as a function of the weight ratio between CS and PMMA.

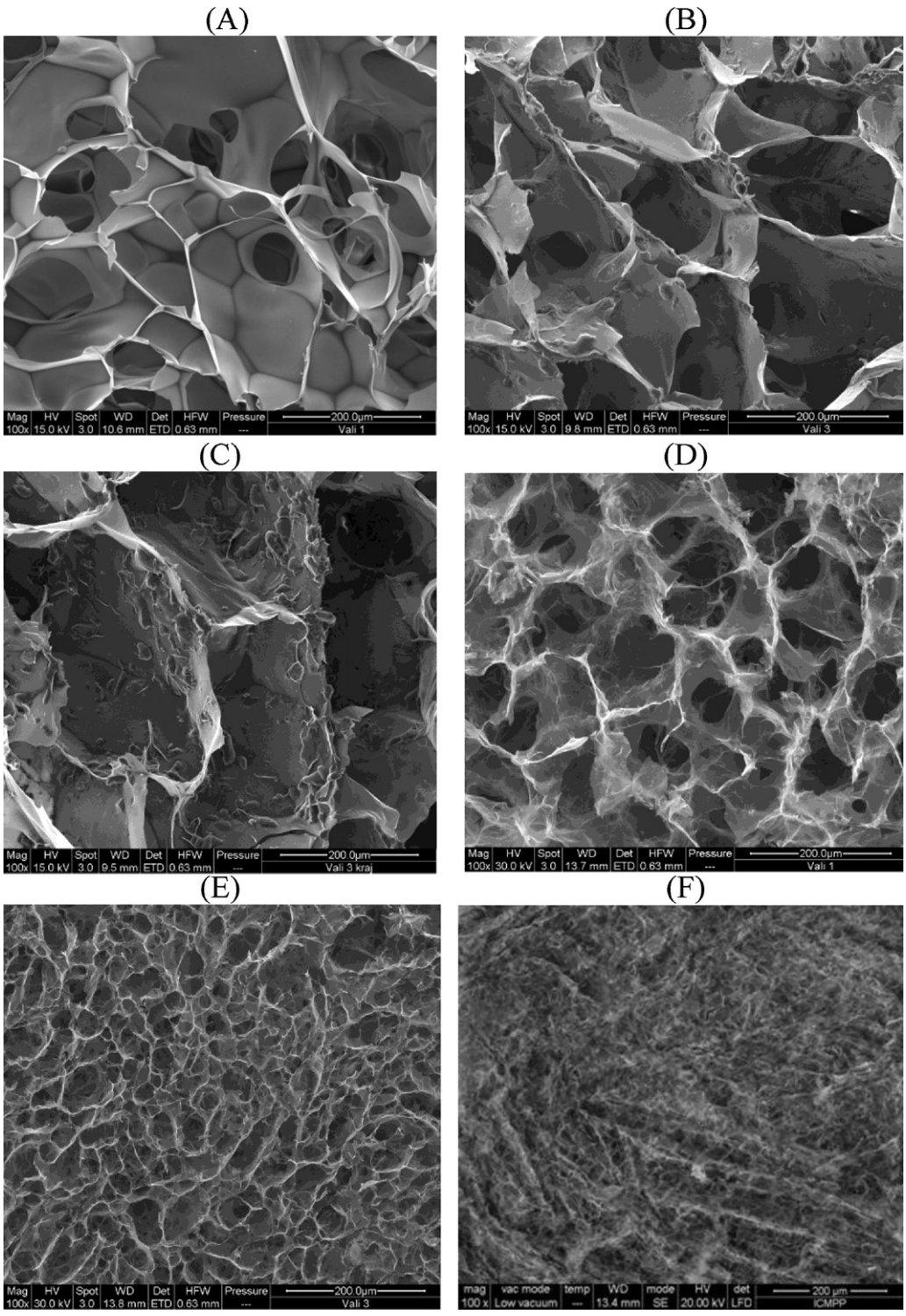

Fig. 2. SEM images of cross-linked CS (A), CS0.5.32 (B), CS2.32 (C), CS6.32 (D), CS25.32 (E) and CS30.32 (F) prepared by conventional ice-templating cross-linking. The scaling bar is 200 μm and magnification = 100×.

The CS cryogels prepared without PMMA exhibit a heterogeneous morphology consisting of polyhedral pores of sizes of about 80 ± 4 μm (cross-linked CS, Fig. 2A), while for those prepared in the presence of PMMA with mesh below 32 μm, the appearance of a second generation of pores with smaller sizes could be observed (Fig. 2B–F). Fig. 2C shows that by increasing the weight ratio between CS and PMMA to 1:2, the presence of small pores in the walls of cryogel is more evident. Also, in the case of the CS cryogels prepared with a weight ratio between CS and PMMA of 1:0.5 (Fig. 2B) or 1:2 (Fig. 2C), the pore walls were very smooth. By increasing the amount of the fractionated PMMA particles to 1:6, CS cryogels with a different internal morphology were obtained, as shown in Fig. 2D. Thus, the pore walls were rough and less compact, the average pore sizes being around 75 ± 3 μm for CS6.32. Further increase of the amount of the fractionated PMMA particles added into the reaction mixture up to 1:25 and 1:30

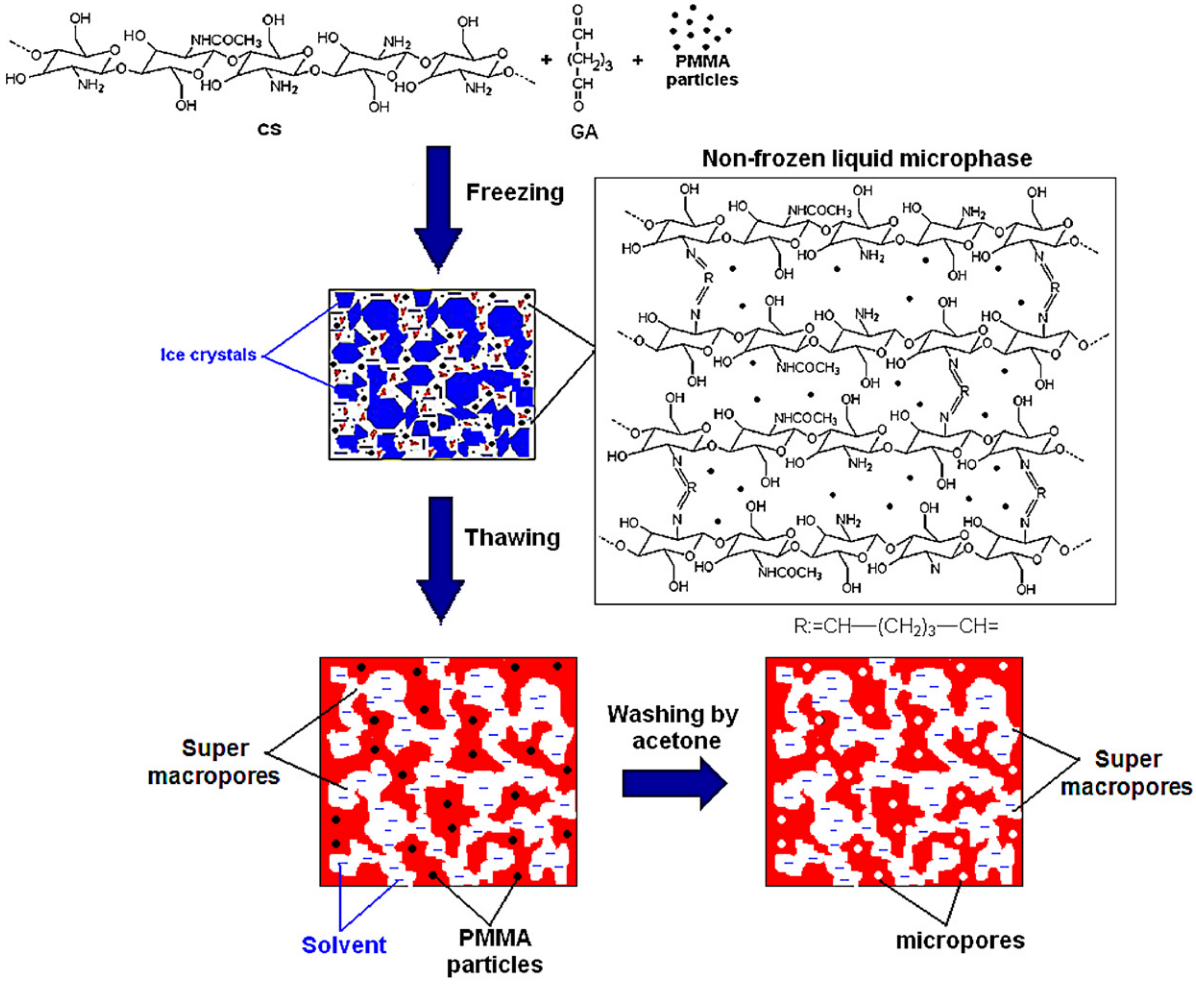

Scheme 1. Schematic representation of the strategy of CS network formation by a combination of the conventional ice-templating process and porogen leaching technique.

conducted to a drastic decrease of the average pore size, as well as to more compact pore walls. As can be observed from Fig. 2E and F, the CS25.32 and CS30.32 cryogels exhibit an average pore size of 35 ± 5 μm and 10 ± 2 μm, respectively.

3.3. *Effect of speed of crystallization on pore structure of cryogels*

Freezing temperature is an important parameter, which remarkably affects formation speed, size and orientation of the solvent crystals (Gutiérrez et al., 2008; Lozinsky, 2002). In our previous study on the cryogel preparation based on PAAm, it was found that the lower the gel preparation temperature, the shorter the time period until the freezing temperature of the reaction mixture was reached (Dinu et al., 2007). In order to see the effect of speed of crystallization on the morphological structure of CS cryogels, two techniques have been used, namely: conventional ice-templating process and unidirectional freezing by liquid nitrogen (−196 °C) or ethylene glycol (−28 °C and −13 °C) as cooling agents.

For conventional ice-templating process, the frozen zones (ice crystals) of the reaction system are produced by the crystal nucleus and grow in all directions, leading to a porous structure by thawing at the end of the gel preparation. The schematic representation of the strategy of CS network formation by a combination of conventional ice-templating process and porogen leaching is depicted in Scheme 1.

As Scheme 1 shows, GA interacts with the amine groups of CS, within the non-frozen liquid microphase, and imine bonds are generated in the final material. The probability as the cross-links to be homogeneous is dependent on the weight ratio between the CS and PMMA used as porogen. During cross-linking of CS by GA at −18 °C, the fractionated PMMA particles could be entrapped within the pore walls of three dimensional network of CS cryogel, and washed out from the cryogel by acetone after reaction, thus leading to a system with porous walls (Scheme 1).

The unidirectional freezing technique presented in this paper for manufacturing aligned-porous cryogels based on CS is different from the conventional ice-templating process. This technique included two steps: in the first step, the reaction mixture containing CS, GA and PMMA as fractionated particles were unidirectional frozen, and in the second step, the frozen systems were transferred to a freezer fixed at −18 °C. In the first step, during the freezing process, the growth of the ice crystals was controlled to orient in one direction parallel to the freezing direction. The cross-linking reaction of CS by GA which takes place at −18 °C (in the second step) is similar with the method used for preparing conventional cryogels (Dinu et al., 2007; Savina et al., 2007). The ice crystals did not melt under this temperature, so the morphology of the oriented ice crystals could be preserved. Finally, after thawing, CS cryogels with aligned pores were obtained.

Morphology of CS cryogels prepared by conventional ice-templating process and unidirectional freezing technique has been analyzed by SEM for two series of samples, prepared with either fractionated PMMA particles with mesh below 32 μm or 50–90 μm. The SEM micrographs taken for CS12.32 and CS12.32LN with a weight ratio between CS and PMMA equal to 1:12, prepared in the presence of the fractionated PMMA particles with mesh below

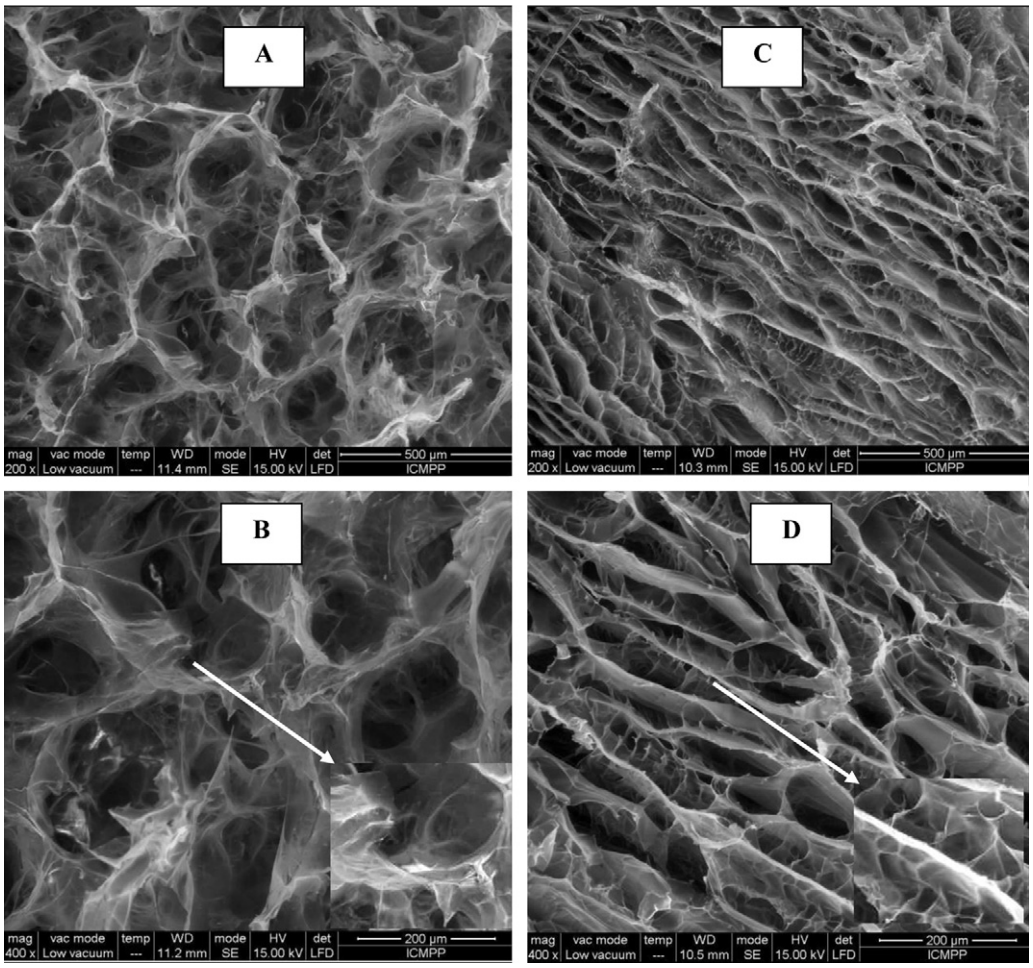

Fig. 3. SEM micrographs of the CS12.32 cryogels prepared by conventional ice-templating cross-linking (A and B) and unidirectional freezing in liquid nitrogen (C and D): (up) the scaling bar 500 μm and magnification = 200×, and (down) the scaling bar 200 μm and magnification = 400×. In the inset of (B) and (D) is evidenced the presence of small pores in the walls of the CS12.32 cryogels.

32 μm, different only by the speed of the crystallization, are presented in Fig. 3.

Fig. 3A and B shows that the conventional CS cryogels (CS12.32) exhibit a heterogeneous morphology consisting of polyhedral pores randomly and evenly distributed, having an average pore diameter of 84 ± 6 μm. Fig. 3C and D shows the internal morphology of the obtained CS cryogels by unidirectional freezing with liquid nitrogen as freezing agent (CS12.32LN). From the cross-sectional view perpendicular to the freezing direction of these CS cryogels, could be observed an oriented structure, which has walls arranged along the freezing direction (Fig. 3C and D) and a honey-comb structure in cross-section, with sizes ranging from 30 μm to 50 μm. Such an aligned porous structure in the freezing direction was also found in the case of the cryogels based on poly(ethylene glycol) with a molecular weight of 700 kDa prepared recently by Wu et al. (2012). It may be concluded that different morphological structures were produced by the different growth of the ice crystals formed in these two techniques. It should be also noted that by cross-linking of CS by GA in the presence of the fractionated PMMA particles with mesh below 32 μm, which have been washed out from the matrix by acetone, pores with sizes of about 10–15 μm were generated in the pore walls of CS cryogels, as shown in the inset of Fig. 3(B) and (D).

SEM micrographs of the CS12.90 cryogels prepared by unidirectional freezing at two temperatures, using EG as cooling agent, are presented in Fig. 4.

As Fig. 4 shows there is a strong influence of the speed of crystallization on the gel morphology. Thus, the cryogel frozen at −13 °C (Fig. 4A and B) display a more irregular distribution of the channels than that frozen at −28 °C (Fig. 4C and D). Furthermore, the distance between the channel walls is around 130 ± 6 μm for the cryogel frozen at −13 °C, and 115 ± 5 μm for that frozen at −28 °C. The difference could be attributed to the freezing duration, which was around 40 min for the gels frozen at −13 °C and around 15 min for the gels frozen at −28 °C (Table 1). It should be taken into account that the reaction mixture frozen at −13 °C has been transferred at a lower temperature for the synthesis of cryogel, while the other has been put at a higher temperature (−18 °C).

3.4. Porosity measurements

Information about the internal structure of all cryogels based on CS in the swollen state was obtained from the relative values of the weight (q_w) and the volume swelling ratios (q_v). During the swelling process, the pores located inside the network are rapidly filled with the solvent; at the same time, the polymer region takes up solvent from the environment, whose extent is depending on the attractive force between the solvent molecules and the polymer segments (Okay, 2000). The equilibrium weight swelling ratio q_w includes the amount of solvent taken by both processes, i.e., q_w includes the solvent in the gel as well as in the pore regions of the network. On the contrary, if we assume isotropic swelling, i.e., the pores volume remains constant upon swelling, volume swelling ratio q_v of porous networks is caused only by the hydration of the network chains. Accordingly, the higher the difference between

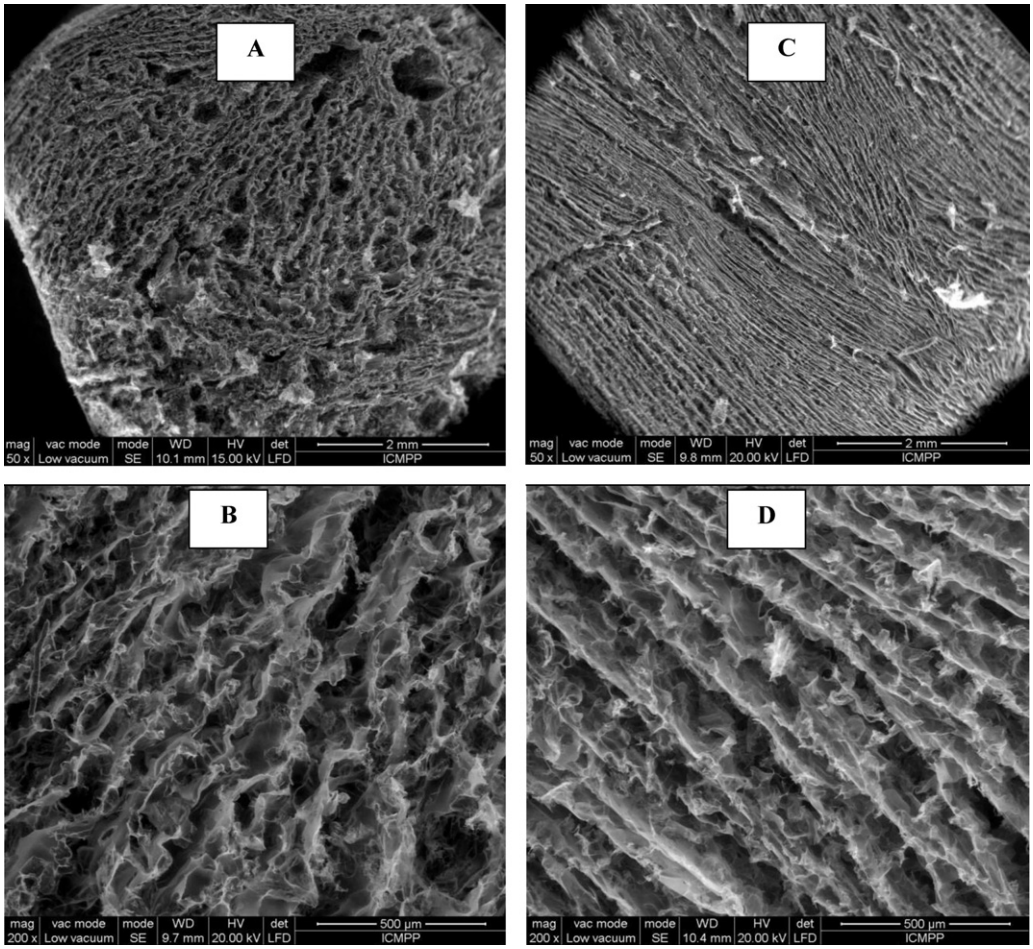

Fig. 4. SEM micrographs of the CS12.90EG cryogels prepared by unidirectional freezing at −13 °C (A and B) and −28 °C (C and D) using ethylene glycol (EG) as cooling agent: (up) the scaling bar 2 mm and magnification = 50×, and (down) the scaling bar 500 μm and magnification = 200×.

q_w and q_v, the higher the volume of pores in the network sample is.

The values of the equilibrium weight swelling ratio (q_w) and the equilibrium volume swelling ratio (q_v) of the CS cryogels are listed in Table 2.

As Table 2 shows, the values of the volume swelling ratio (q_v) range from 1.056 to 1.85 and the values of the equilibrium weight swelling ratio (q_w) range from 40.84 to 59.111, suggesting the appearance of pores in the gel matrices prepared at −18 °C.

Table 2
Comparison of the swollen state porosity (P_s), dry-state porosity (P), and volume fraction of pores (V_p) for cross-linked CS cryogel and CS cryogels prepared in the presence of the fractionated PMMA particles.

Sample code	q_v[a]	q_w[b]	P_s[c] (%)	P[d] (%)	V_p[e] (g/cm^3)
CS	1.258	40.84	97.05	94.866	0.958
CS0.5.32	1.115	42.07	97.31	95.358	0.960
CS2.32	1.056	53.062	97.83	96.676	0.965
CS6.32	1.559	43.021	96.69	94.05	0.960
CS12.32	1.517	48.732	96.914	94.88	0.965
CS12.32LN	1.588	50.623	97.101	94.84	0.967
CS12.50	1.134	51.032	97.4	96.34	0.962
CS12.90	1.208	58.47	98.16	97.168	0.970
CS25.32	1.507	56.16	96.94	95.58	0.959
CS30.32	1.85	59.111	97.98	94.84	0.953

[a] The equilibrium volume swelling ratio was calculated by Eq. (4).
[b] The equilibrium weight swelling ratio was calculated by Eq. (5).
[c] The swollen state porosity was evaluated by Eq. (3).
[d] The dry-state porosity was determinated by Eq. (8).
[e] The volume fraction of pores was estimated by Eq. (9).

From the weight and volume swelling ratios of hydrogels, the swollen state porosity of the networks, P_s, was estimated using Eq. (3) and the results are shown in Table 2. The swollen state porosity P_s is about 97% with no big difference between the CS cryogels prepared with or without PMMA. It may be concluded that, for these weight ratios, the formation of pores by ice-templated process predominates over the formation of pores due to the presence of PMMA as porogen. Moreover, in Table 2 are presented the dry-state porosities P of the networks and volume fraction of pores in network (V_p) calculated by Eqs. (8) and (9). The three different techniques used to estimate the porosity of the networks, gave similar results for the CS cryogels prepared with or without fractionated PMMA particles. The dry-state porosity P is slightly lower than the swollen state porosity P_s, probably due to the partial collapse of the pores during drying. The results obtained by porosity measurements are in agreement with the SEM analysis of cryogel networks morphology in dry state (Figs. 1–3).

4. Conclusions

The preparation of cryogels based on CS with tailored morphology by the synthesis conditions is described first in this paper. The morphology of cryogels has been strongly influenced by: (1) the mesh of the fractionated PMMA particles (2) the weight ratio between CS and fractionated PMMA particles, and (3) the speed of the crystallization. Thus, CS cryogels having a heterogeneous morphology with randomly and evenly distributed polyhedral pores have been designed by a strategy, which combines conventional

ice-templating process and porogen leaching. The pore sizes and the pore walls morphology of CS cryogels were first tailored by the mesh of the fractionated PMMA particles. For the same weight ratio between CS and PMMA (1:12), and mesh of PMMA ranging from below 32 μm to 50–90 μm, a decrease of the pores sizes from 84 ± 6 μm to 60 ± 4 μm, as well as an increase of the number of the interconnected small pores has been found. It was observed that with the increase of the weight ratio between CS and fractionated PMMA particles with mesh below 32 μm from 1:12 to 1:30, the average size of the interconnected pores decreased from 84 ± 6 μm to 10 ± 2 μm.

Using the unidirectional freezing technique, CS cryogels with aligned walls along the freezing direction have been generated. It was observed that the speed of crystallization had a strong influence on the gel morphology, the cryogels frozen at −13 °C exhibiting a more irregular distribution of the channels than that frozen at −28 °C, the distance between the channel walls being around 130 ± 6 μm for the cryogels frozen at −13 °C, and 115 ± 5 μm for that frozen at −28 °C. The cryogels synthesized in this work would be of interest as potential scaffolds for cell growth, the presence of less compact walls between the large pores being favorable for the diffusion of low-molecular substances.

Acknowledgments

This work was supported by CNCSIS-UEFISCSU by the project PN-II-ID-PCE-2011-3-0300 and Grant Agency of the Czech Republic, projects No. 108/12/1538.

References

Aranaz, I., Mengíbar, M., Harris, R., Paños, I., Miralles, B., Acosta, N., et al. (2009). Functional characterization of chitin and chitosan. *Current Chemical Biology*, *3*, 203–230.

Bajpai, A. K., Shukla, S. K., Bhanu, S., & Kankane, S. (2008). Responsive polymers in controlled drug delivery. *Progress in Polymer Science*, *33*, 1088–1118.

Baydemir, G., Bereli, N., Andac, M., Say, R., Galaev, I. Y., & Denizli, A. (2009). Bilirubin recognition via molecularly imprinted supermacroporous cryogels. *Colloid and Surfaces B: Biointerfaces*, *68*, 33–38.

Brugnerotto, J., Lizardi, J., Goycoolea, F. M., Argüelles-Monal, W., Desbriéres, J., & Rinaudo, M. (2001). An infrared investigation in relation with chitin and chitosan characterization. *Polymer*, *42*, 3569–3580.

Chang, C., Duan, B., & Zhang, L. (2009). Fabrication and characterization of novel macroporous cellulose–alginate hydrogels. *Polymer*, *50*, 5467–5473.

Dinu, M. V., Ozmen, M. M., Drăgan, E. S., & Okay, O. (2007). Freezing as a path to build macroporous structures: Superfast responsive polyacrylamide hydrogels. *Polymer*, *48*, 195–204.

Dinu, M. V., Perju, M. M., & Drăgan, E. S. (2011a). Porous semi-interpenetrating hydrogel networks based on dextran and polyacrylamide with superfast responsiveness. *Macromolecular Chemistry and Physics*, *212*, 240–251.

Dinu, M. V., Perju, M. M., & Drăgan, E. S. (2011b). Composite IPN ionic hydrogels based on polyacrylamide and dextran sulfate. *Reactive Functional Polymers*, *71*, 881–890.

Dispinar, T., Van Camp, W., De Cock, L. J., De Geest, B. G., & Du Prez, F. E. (2012). Redox-responsive degradable PEG cryogels as potential cell scaffolds in tissue engineering. *Macromolecular Bioscience*, *12*, 383–394.

Dragan, E. S., Cazacu, M., & Nistor, A. (2009). Ionic organic/inorganic materials. III. Stimuli responsive hybrid hydrogels based on oligo(N,N-dimethylaminoethylmethacrylate) and chloroalkyl-functionalized siloxanes. *Journal of Polymer Science Part A Polymer Chemistry*, *47*, 6801–6813.

Dragan, E. S., & Perju, M. M. (2010). Preparation and swelling behavior of chitosan/poly(N-2-aminoethyl acrylamide) composite hydrogels. *Soft Materials*, *8*, 49–62.

Dragan, E. S., Perju, M. M., & Dinu, M. V. (2012). Preparation and characterization of IPN composite hydrogels based on polyacrylamide and chitosan and their interaction with ionic dyes. *Carbohydrate Polymers*, *88*, 270–281.

Gamzazade, A. I., Shimac, V. M., Skljar, A. M., Stykova, E. V., Pavlova, S. A., & Rogozin, S. V. (1985). Investigation of the hydrodynamic properties of chitosan solutions. *Acta Polymerica*, *36*, 420–424.

Gutiérrez, M. C., Ferrer, M. L., & del Monte, F. (2008). Ice-templated materials: Sophisticated structures exhibiting enhanced functionalities obtained after unidirectional freezing and ice-segregation-induced self-assembly. *Chemistry of Materials*, *20*, 634–648.

Hobzova, R., Pradny, M., Zhunusbekova, N. M., Sirc, J., Guryca, V., & Michalek, J. (2011). Bioactive support for cell cultivation and potential grafting. Part 1: Surface modification of 2-hydroxyethyl methacrylate hydrogels for avidin immobilization. *e-Polymers*, *043*, 1–17.

Hu, X. X., Shen, H., Yang, F., Bei, J. Z., & Wang, S. G. (2008). Preparation and cell affinity of microtubular orientation-structured PLGA(70/30) blood vessel scaffold. *Biomaterials*, *29*, 3128–3136.

Ji, C., Annabi, N., Khademhosseini, A., & Dehghani, F. (2011). Fabrication of porous chitosan scaffolds for soft tissue engineering using dense gas CO_2. *Acta Biomaterialia*, *7*, 1653–1664.

Kathuria, N., Tripathi, A., Kar, K. K., & Kumar, A. (2009). Synthesis and characterization of elastic and macroporous chitosan–gelatin cryogels for tissue engineering. *Acta Biomaterialia*, *5*, 406–418.

Kim, D., & Park, K. (2004). Swelling and mechanical properties of superporous hydrogels of poly(acrylamide-co-acrylic acid)/polyethylenimine interpenetrating polymer networks. *Polymer*, *45*, 189–196.

Kim, J. W., Taki, K., Nagamine, S., & Ohshima, M. (2009). Preparation of porous poly(L-lactic acid) honeycomb monolith structure by phase separation and unidirectional freezing. *Langmuir*, *25*, 5304–5312.

Kirsebom, H., Topgaard, D., Galaev, I., & Yu Mattiasson, B. (2010). Modulating the porosity of cryogels by influencing the nonfrozen liquid phase through the addition of inert solutes. *Langmuir*, *26*, 16129–16133.

Lesný, P., Prádný, M., Jendelová, P., Michálek, J., Vacík, J., & Syková, E. (2006). Macroporous hydrogels based on 2-hydroxyethyl methacrylate. Part 4. Growth of rat bone arrow stromal cells in three-dimensional hydrogels with positive and negative surface charges and in polyelectrolyte complexes. *Journal of Materials Science: Materials in Medicine*, *17*, 829–833.

Lozinsky, V. I. (2002). Cryogels on the basis of natural and synthetic polymers: Preparation, properties and application. *Russian Chemical Reviews*, *71*, 489–511.

Lozinsky, V. L., Plieva, F. M., Galaev, I. Y., & Mattiasson, B. (2001). The potential of polymeric cryogels in bioseparation. *Bioseparation*, *10*, 163–188.

Mukai, R., Nishihara, H., & Tamon, H. (2008). Morphology maps of ice-templated silica gels derived from silica hydrogels and hydrosols. *Microporous and Mesoporous Materials*, *116*, 166–170.

Okay, O. (2000). Macroporous copolymer networks. *Progress in Polymer Science*, *25*, 711–779.

Orakdogen, N., Karacan, P., & Okay, O. (2011). Macroporous, responsive DNA cryogel beads. *Reactive Functional Polymers*, *71*, 782–790.

Peppas, N. A., Hilt, J. Z., Khademhosseini, A., & Langer, R. (2006). Hydrogels in biology and medicine: From molecular principles to bionanotechnology. *Advanced Materials*, *18*, 1345–1360.

Přádný, M., Lesny, P., Fiala, J., Vacik, J., Sloui, M., Michálek, J., et al. (2003). Macroporous hydrogels based on 2-hydroxyethyl metacrylate. Part 1. Copolymers of 2-hydroxyethyl metacrylate with methacrylic acid. *Collection of Czechoslovak Chemical Communications*, *68*, 812–822.

Přádný, M., Šlouf, M., Martinová, L., & Michálek, J. (2010). Macroporous hydrogels based on 2-hydroxyethyl metacrylate. Part 7: Methods of preparation and comparison of resulting physical properties. *e-Polymers*, *043*, 1–12.

Reis, A. V., Guilherme, M. R., Moia, T. A., Mattoso, L. H. C., Muniz, E. C., & Tambourgi, E. B. (2008). Synthesis and characterization of a starch-modified hydrogel as potential carrier for drug delivery system. *Journal of Polymer Science Part A Polymer Chemistry*, *46*, 2567–2574.

Savina, I. N., Cnudde, V., D'Hollander, S., Van Hoorebeke, L., Mattiasson, B., Galaev, I. Y., et al. (2007). Cryogels from poly(hydroxyethyl methacrylate): Macroporous, interconnected materials with potential as cell scaffolds. *Soft Matter*, *3*, 1176–1184.

Sayil, C., & Okay, O. (2001). Macroporous poly(N-isopropyl)acrylamide networks: Formation conditions. *Polymer*, *42*, 7639–7652.

Shapiro, L., & Cohen, S. (1997). Novel alginate sponges for cell culture and transplantation. *Biomaterials*, *18*, 583–590.

Takei, T., Nakahara, H., Ijima, H., & Kawakami, K. (2012). Synthesis of a chitosan derivative soluble at neutral pH and gellable by freeze–thawing, and its application in wound care. *Acta Biomaterialia*, *8*, 686–693.

Wu, J., Zhao, Q., Sun, J., & Zhou, Q. (2012). Preparation of poly(ethylene glycol) aligned porous cryogels using a unidirectional freezing technique. *Soft Matter*, *8*, 3620–3626.

Zhao, Q., Sun, J., Wu, X., & Lin, Y. (2011). Macroporous double-network cryogels: Formation mechanism, enhanced mechanical strength and temperature/pH dual sensitivity. *Soft Matter*, *7*, 4284–4293.